

# Kinetic study of corrosion product activity in primary coolant pipes of a typical PWR under flow rate transients and linearly increasing corrosion rates

Muhammad Rafique, Nasir M. Mirza <sup>\*</sup>, Sikander M. Mirza

*Department of Physics and Applied Mathematics, Pakistan Institute of Engineering and Applied Sciences,  
Nilore, Islamabad 45650, Pakistan*

Received 6 December 2002; accepted 6 July 2005

## Abstract

Transient behavior of activated corrosion products on inner surfaces of primary coolant pipes have been studied for a typical pressurized water reactor (PWR) under flow rate perturbations and linearly increasing corrosion rate conditions. Computer program CPAIR-P [27] has been modified to accommodate for time dependent corrosion rates. Results, for  $^{24}\text{Na}$ ,  $^{56}\text{Mn}$ ,  $^{59}\text{Fe}$ ,  $^{58}\text{Co}$ ,  $^{60}\text{Co}$  and  $^{99}\text{Mo}$ , show that the specific activity in primary loop approaches equilibrium value under normal operating conditions fairly rapidly. Predominant corrosion product activity during operation is due to  $^{56}\text{Mn}$  while  $^{58}\text{Co}$  and  $^{60}\text{Co}$  dominate the activity after shutdown of reactor. Flow rate perturbations for various linearly increasing corrosion rates were introduced in the system and effects on saturation activity were studied. For a linear decrease in flow rate and a constant corrosion rate, the total coolant activity and activity on pipe scale approaches higher saturation values as compared to the normal condition values. With a linearly increasing corrosion rate, the behavior of specific activity changes considerably and the effect of flow rate perturbations on specific activity for pipe scale is smeared by a linearly rising corrosion rates. The saturation value of activity depends on both the changes in flow rate ( $\Delta w$ ) and equilibrium corrosion rate ( $C_s$ ) values while, the time taken to reach the saturation activity depends on the slope of corrosion rate. The peak value and the subsequent decay of the corrosion product activity after scram is a strong function of flow rate and efficiencies to remove corrosion products from pipe scale.

© 2005 Elsevier B.V. All rights reserved.

## 1. Introduction

A total of around 2800 TW h energy amounting to ~16% of the global electricity supply is generated by 441 nuclear reactors operating in 31 countries world-

wide. The pressurized water reactors (PWRs) accounts for two-third majority of these nuclear power plants. In these systems, the fuel cladding corrosion is of major concern to-date. Also, irradiation assisted stress corrosion cracking of core-shroud baffle bolts has recently been observed in some PWRs and advanced water chemistry modifications are being considered with regard to minimization of the activity buildup [1]. Although, in recent past, the maintenance dose rates show a steady decline, it remains a challenge for LWRs

<sup>\*</sup> Corresponding author. Tel.: +92 51 9290272–4/2208016; fax: +92 51 9223727.

E-mail address: [nasirmm@yahoo.com](mailto:nasirmm@yahoo.com) (N.M. Mirza).

to reduce it by about two orders of magnitude to come down to the prevailing level for gas- or sodium-cooled power plants. The estimated penalties, due to prolongation and reduced effectiveness of maintenance in the case of LWRs, are already of the order of several million dollars annually [2].

In PWRs, there are three main sources of radioactive contamination: (i) fission products and actinides leaking out of fuel pins, (ii) coolant activation due to irradiation and (iii) activated corrosion products [3,4]. Out of these, the activated corrosion products dominate the post-shutdown activity. The corrosion products are formed due to liquid–metal interaction and various constituents of cladding and piping are released as corrosion products which are carried into reactor core by coolant flow and become radioactive as a result of neutron irradiation. These are deposited at various places in the primary circuit of PWRs and may be released again in turbulent coolant flows. Clearly the coolant activity due to corrosion products is dependant on corrosion rates, flow rates, deposition and release of corrosion products.

In past, a number of experimental as well as theoretical studies have been carried out in order to study the formation, activation, deposition and re-release of corrosion products. Initially, experimental efforts were focused on deposition of corrosion products in turbulent flows [5,6]. Efforts have also been made to model transport of corrosion products in PWR primary loops and various computer programs have been developed for this purpose. These programs typically carryout detailed modeling of some aspects of the problem. The PAC-TOLE [7] and CORA [8] are examples of such efforts. Lately, attention has been focused on in-pile measurements of corrosion transport studies [9].

The severity of corrosion product formation problem has grown due to changing trends towards high burnup and/or higher power fuel which has higher potential for crud deposition [10]. Furthermore, the corrosion rates have been found to exhibit increasing behavior with the operation time [11–13].

For PWRs under normal conditions, the corrosion product activity is dominated by the short-lived  $^{56}\text{Mn}$  and  $^{24}\text{Na}$ . Nearly all the long-lived activity in the coolant is due to iron, molybdenum and cobalt with most significant radionuclides as  $^{59}\text{Fe}$ ,  $^{99}\text{Mo}$ ,  $^{58}\text{Co}$  and  $^{60}\text{Co}$ . Various nuclear properties of these nuclides are shown in Table 1 [14]. The  $^{55}\text{Mn}$  has an activation cross-section of  $13.4b$  for the thermal neutrons to produce  $^{56}\text{Mn}$ . The neutron activation of structural  $^{27}\text{Al}$  and activation of  $^{23}\text{Na}$  from salt impurities in water can produce  $^{24}\text{Na}$ . The use of high-purity water, demineralization of water and the presence of filters keep the amount of dissolved salts to less than 0.05 ppm [14]. It was seen for low powered nuclear plants, having large aluminum fraction in the system, the coolant activity due to  $^{24}\text{Na}$  remained comparable to  $^{16}\text{N}$  activity [15,16]. It was also shown in subsequent experimental studies that the effect of sodium salt as an impurity in coolant remains small as compared to  $^{24}\text{Na}$  resulting from aluminum activation [17]. However, the half lives of all corrosion products remains more than 2 h. Therefore, the primary coolant will always retain activity for several hours even after the reactor shutdown and any transient condition during operation can further increase the coolant activity.

The turbulent flow of coolant in primary coolant loop keeps on depositing activated nuclides as it passes through the flow channels of the primary coolant loop. These deposits of dissolved and suspended radionuclides on the scale of primary circuit's inner surfaces do pose

Table 1  
Typical activation products found in PWRs and their reaction properties

Corrosion product	Reaction and neutron energy	Activation cross-section and half-life	$\gamma$ -Ray energy (MeV) and % yield
$^{24}\text{Na}$	$^{27}\text{Al}(n,\alpha)^{24}\text{Na}$ ( $E_n > 11.6$ MeV)	$6 \times 10^{-4}b$ (15.4 h)	4.1 (100%)
	$^{23}\text{Na}(n,\gamma)^{24}\text{Na}$ ( $E_n$ is thermal)	$0.53b$ (15.4 h)	
$^{56}\text{Mn}$	$^{55}\text{Mn}(n,\gamma)^{56}\text{Mn}$ (Thermal neutrons)	$13.4b$	2.13 (15%)
		(2.58 h)	1.81 (24%)
$^{59}\text{Fe}$	$^{58}\text{Fe}(n,\gamma)^{59}\text{Fe}$ (Thermal neutrons)	$0.9b$	1.17 (99.9%)
		45.1 h	1.33 (99.9%)
$^{58}\text{Co}$	$^{58}\text{Ni}(n, p)^{58}\text{Co}$ (Fast neutrons)	$0.146b$ (70.88 d)	–
$^{60}\text{Co}$	$^{59}\text{Co}(n,\gamma)^{60}\text{Co}$	$20b$	1.173 (99.9%)
		(5.3 years)	1.332 (99.9%)
$^{99}\text{Mo}$	$^{98}\text{Mo}(n,\gamma)^{99}\text{Mo}$ $E_n > 3.1$ MeV	$0.45b$	0.78 (8%)
		(67.0 h)	0.74 (8%)

maintenance issues. Chemical procedures to find amounts of corrosion products in primary coolants of PWRs after shutdown were studied by Raymond and his colleagues for both target and active nuclides. They showed that detection limits are between 0.05 and 0.3 mg/L for undissolved species and for ions these are in the range of 0.03–0.14 mg/L for sample volumes of 0.5 L [18]. Recently Hirschberg and his colleagues have also experimentally studied accumulation of radioactive corrosion products on steel surfaces of VVER type nuclear reactors for  $^{60}\text{Co}$  buildup on steel surfaces [12,13]. Effects of corrosion inhibitors, on corrosion rates for carbon steel, were also studied by Dey and his co-workers and they proposed high efficiency organic inhibitors for base metal protection [11].

Operating parameters of the reactor also affect strongly the types of radionuclides formed, the levels of saturation activity reached and the rates at which the saturation is reached. These include the composition of the materials in contact with the coolant, amount and the types of the impurities present in the coolant, reactor power, residence time of coolant in core, temperatures and pressure, coolant flow rates, corrosion rates, filter efficiency and deposition rates of radioactive elements.

During the past decade many studies were conducted on coolant activation with specific interest to find effects of flow rate and power perturbation on dose rate in medium flux research reactors [15,16]. Calculations of coolant activation were also done for low flux natural convection based systems [19,20]. Experimental measurements of  $^{24}\text{Na}$  activity in low power research reactors yielded that majority of  $^{24}\text{Na}$  comes from neutron activation of  $^{27}\text{Al}$  and its subsequent mixing in coolant and it is second important contributor to the total dose after  $^{16}\text{N}$  in coolant activity [21]. It was seen in simulations of low and high flux systems that transients under reactivity and loss of flow do lead to peaking of neutron flux in reactor and production of high activity in coolant [22–24]. These strongly affect the coolant activity and corrosion rate. Sensitivity analysis of reactivity insertion limits with respect to safety parameters in typical MTRs showed that neutron flux peaking and clad melting conditions are dictated by void coefficients, transient type and their rates [25]. Void coefficient, Doppler coefficient and temperature of moderator showed significant effects on power peaking in a non-uniform manner within the core. It also led to the necessity of performing detailed space and time calculations of flux for conditions [26].

Modeling of corrosion products activity in primary coolants of PWRs under flow rate perturbations were also done to investigate effects due to flow coastdown [17]. A computer code CPAIR was developed in FORTRAN-77 to calculate specific activity due to corrosion products in primary water of light water reactors. It was shown that minimum value of coolant activity depends strongly on the slope of linear decrement of flow rate.

The program was further improved to incorporate the effect of power perturbations on corrosion product activity in coolants of a PWR [27]. The computer code was modified as CPAIR-P and effects of fast and slow transients were studied on dose rates due to corrosion activity in coolant. All these studies assumed a constant and uniform corrosion rate during and after transients. However, the corrosion rate does increase slowly with plant operating at full power; it also increases with temperature and pressure. The rate of increase of corrosion depends on integrated effect of neutron flux, time of reactor operation and reactor temperatures [28,29].

Calculations of corrosion product activity on inner surfaces of primary coolant piping are presented in this work, when corrosion rate is linearly rising in the primary circuit. These changes are furthermore superimposed on flow rate perturbations. The computer program CPAIR-P [24,27] was modified to incorporate both the linearly increasing corrosion and flow rate perturbations. Calculations for specific activity due to  $^{24}\text{Na}$ ,  $^{56}\text{Mn}$ ,  $^{59}\text{Fe}$ ,  $^{58}\text{Co}$  and  $^{99}\text{Mo}$  in the coolant and on primary pipe scale have been done. First, we compared the total activity for a uniform and fixed corrosion rate under different flow rate transients in a PWR. Then, both increasing corrosion rates and different types of flow rate perturbations were introduced and the behavior of corrosion product activity on primary pipe scale was studied. Results for fast and slow corrosion increase and flow rate perturbations are discussed in this paper.

## 2. Mathematical model

The time dependent concentration comes from a balance between the rate of production of radioactive nuclei and the rate at which they are lost as a result of purification, deposition on surfaces, leakage and radioactive decay. Possible paths leading to various productions and losses of corrosion products are shown in Fig. 1. We have assumed a uniform time dependent corrosion in the coolant circuit and have ignored the space distribution effects. The deposition of the activity on surfaces in contact with the cooling water is proportional to the concentration of the corrosion products in water. Ion exchangers and filters are assumed to remove impurities in proportion to their concentration in the coolant.

The concentration of target nuclides in the primary coolant water, on the inner walls of the piping and on the core surfaces have been denoted by  $N_w$ ,  $N_p$  and  $N_c$  respectively in atoms/cm<sup>3</sup>. Also the concentrations of the activated nuclides in primary water, on the piping and on the core have been represented by  $n_w$ ,  $n_p$  and  $n_c$  respectively, in atoms/cm<sup>3</sup>. Then the net rate of change of active material concentration in primary coolant is given by the difference of the production and the loss rates [17,27] in Eq. (1). The first term on right-hand

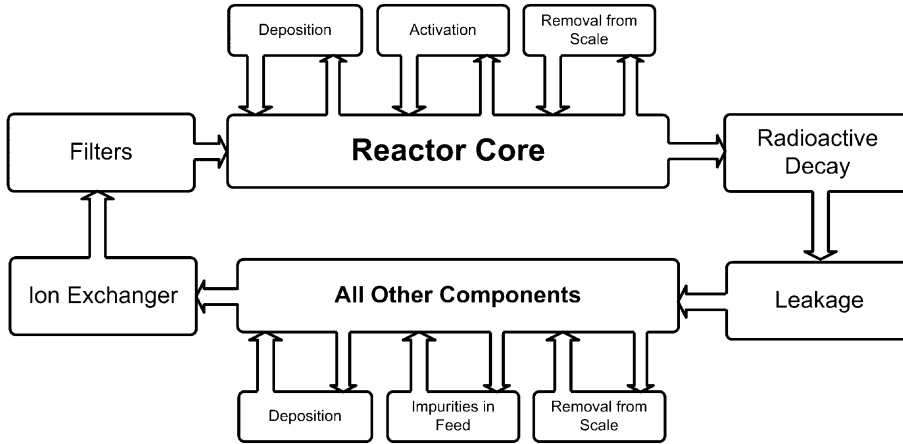


Fig. 1. Production and loss paths for corrosion products in primary coolant circuit of a typical PWR.

side gives the production rate due to neutron flux, the second term gives loss rates due to removal by ion-exchanger, deposition on pipes, deposition on core surfaces and removal by filters; the third term gives loss rate due to various leakages whereas the fourth and the fifth terms are production rates due to scales and from core surfaces:

$$\frac{dn_w}{dt} = \sigma\phi_\epsilon N_w - \left\{ \sum_j \frac{\epsilon_j Q_j g(t)}{V_w} + \sum_k \frac{l_k g(t)}{V_w} + \lambda \right\} n_w + \frac{K_p g(t)}{V_w} n_p + \frac{K_c g(t)}{V_w} n_c, \quad (1)$$

where  $\sigma$  is the group constant for the production of isotope from target nuclide;  $\phi_\epsilon$  is the effective group flux (neutrons per  $\text{cm}^2$  per s);  $N_w$  is the target nuclide concentration in water (in atoms per  $\text{cm}^3$ ). The sum over  $j$  for  $\epsilon_j Q_j$  is given as following:

$$\sum_j \epsilon_j Q_j = \epsilon_I Q_I + \epsilon_p Q_p + \epsilon_c Q_c + \epsilon_F Q_F, \quad (2)$$

where the quantities  $\epsilon_I Q_I$ ,  $\epsilon_p Q_p$ ,  $\epsilon_c Q_c$  and  $\epsilon_F Q_F$  are removal rates due to ion exchanger, deposition on pipes, deposition on core surfaces and removal by filters, respectively. The term  $l_k$  is the rate at which primary coolant loop loses water from its  $k$ th leak (in  $\text{cm}^3$  per second);  $K_p$  and  $K_c$  are rates at which isotopes are removed from the scale on piping ( $\text{cm}^3$  per second) and from the core (in  $\text{cm}^3$  per second) respectively. For a typical PWR the measured values of these removal rates are shown in Table 2. The first term on left-hand side of Eq. (1), represents the production of radioactive isotopes. The second term is the rate at which the active nuclides are lost as a result of purification by the ion-exchanger and filters, deposition on the piping and core and decay. The third and fourth terms are the rates at which the activity is re-introduced into the coolant by

Table 2  
Experimental values of exchange rates in a typical PWR<sup>a</sup>

Rate type	Value
Deposition on core ( $\epsilon_c Q_c$ )	80.0 $\text{cm}^3$ per second
Deposition on piping ( $\epsilon_p Q_p$ )	13.7 $\text{cm}^3$ per second
Ion-exchanger removal ( $\epsilon_I Q_I$ )	500–781 $\text{cm}^3$ per second
Re-solution ratio for core ( $K_c$ )	40.0 $\text{cm}^3$ per second
Re-solution ratio for piping ( $K_p$ )	6.9 $\text{cm}^3$ per second
Volume of primary coolant ( $V_w$ )	$1.37 \times 10^7 \text{ cm}^3$
Volume of scale on core ( $V_c$ )	$9.08 \times 10^6 \text{ cm}^3$
Volume of scale on piping ( $V_p$ )	$1.37 \times 10^6 \text{ cm}^3$
Total corrosion surface ( $S$ )	$1.01 \times 10^8 \text{ cm}^2$

<sup>a</sup> Refs. [14,29].

erosion from scale on piping and the core. To include any flow rate perturbation we define a parameter  $g(t)$ :

$$g(t) = w(t)/w_0, \quad (3)$$

where  $w_0$  is the steady state flow rate under normal operations and  $w(t)$  is the time dependent flow rate. The averaged neutron flux for a given energy group is also affected by the flow rate changes as

$$\phi_\epsilon = \phi_0 \left\{ \frac{1 - \exp(-\lambda T_c)}{1 - \exp(-\lambda T_L)} \right\}. \quad (4)$$

The values of decay constant ( $\lambda$ ) for isotopes of interest are provided in Table 1. The group flux  $\phi_0$  is averaged over the geometry of the core and have been estimated using programs LEOPARD [30] and ODMUG [31] in the code CPAIR-P as subroutines. The time  $T_c$  and  $T_L$  are the core residence time and loop time (required to complete the primary loop once) respectively. The core residence time is

$$T_c = \frac{H\rho A}{w(t)}, \quad (5)$$

where  $H$  is the core height;  $A$  is the flow cross-sectional area in  $\text{cm}^2$ ;  $\rho$  is the coolant density at operating temperatures and  $w(t)$  is the time dependent flow rate (g per second). The loop time is approximated as  $L_p T_c / H$  for the complete loop length  $L_p$ .

The rate of build-up of target nuclide concentration in coolant water can be written as

$$\frac{dN_w}{dt} = - \left\{ \sum_j \frac{\varepsilon_j Q_j g(t)}{V_w} + \sum_k \frac{l_k g(t)}{V_w} + \sigma \phi_e \right\} N_w + \frac{K_p g(t)}{V_w} N_p + \frac{K_c g(t)}{V_w} N_c + S_w, \quad (6a)$$

$$S_w = \frac{C(t)S}{V_w} \frac{N_0}{A} f_n f_s, \quad (6b)$$

where  $N_p$  is concentration of target nuclide on the piping;  $N_c$  is concentration of target on the core, and  $S_w$  is the source term for corrosion. The  $C(t)$  is the time dependent corrosion rate (g per  $\text{cm}^2$  per s);  $S$  is the area of system exposed to coolant for corrosion;  $N_0$  is Avogadro's number ( $6.023 \times 10^{23}$  atoms per g mole) and  $A$  is the atomic weight of the target nuclide (g). Here,  $f_n$  and  $f_s$  are abundances of target nuclide and chemical element in the system respectively.

The impurity removal by ion-exchanger, core deposition and leakage are directly related to the flow rate. Also, the rate of re-entry from scales is directly proportional to the primary coolant flow rate. Therefore the rate of activity build-up on the core scale is given by

$$\frac{dn_c}{dt} = \sigma \phi_0 N_c + \frac{\varepsilon_c Q_c g(t)}{V_c} n_w - \left\{ \frac{K_c g(t)}{V_c} + \lambda \right\} n_c, \quad (7)$$

where  $V_c$  is volume of the scale on the core ( $\text{cm}^3$ ) and  $\phi_0$  is thermal neutron flux average over the geometry of the core (neutrons/ $\text{cm}^2$  s).

The rate of buildup of target nuclide concentration on the core scale ( $N_c$ ) is given by the following equation:

$$\frac{dN_c}{dt} = \frac{\varepsilon_c Q_c g(t)}{V_c} N_w - \left\{ \frac{K_c g(t)}{V_c} + \sigma \phi_0 \right\} N_c. \quad (8)$$

The rate of deposition of active material on the piping scaling ( $n_p$ ) can be obtained from following balance:

$$\frac{dn_p}{dt} = \frac{\varepsilon_p Q_p g(t)}{V_p} n_w - \left\{ \frac{K_p g(t)}{V_p} + \lambda \right\} n_p, \quad (9)$$

where  $V_p$  is the volume of scale on the piping ( $\text{cm}^3$ ). Then the rate of change of target nuclide on piping walls ( $N_p$ ) is

$$\frac{dN_p}{dt} = \frac{\varepsilon_p Q_p g(t)}{V_p} N_w - \frac{K_p g(t)}{V_p} N_p. \quad (10)$$

Based on the above system of Eqs. (1)–(10) the computer program CPAIR-P (Corrosion Product Activity in Reactors) [27] was modified for this work to include the effect of both increasing corrosion rate and flow rate

Table 3  
Typical design specifications of a PWR

Parameter	Value
Specific power (MW(th)/kg U)	33
Power density (MW(th)/ $\text{m}^3$ )	102
Core height (m)	4.17
Core diameter (m)	3.37
No. of assemblies	194
Rods per assembly	264
Fuel type	UO <sub>2</sub>
Clad type	Zircaloy
Lattice pitch (mm)	12.6
Fuel rod outer diameter (mm)	9.5
Average enrichment (w%)	3.0
Flow rate (Mg/s)	18.3
Linear heat rate (kW/ $\text{m}^2$ )	17.5
Coolant pressure (MPa)	15.5
Inlet Coolant temperature ( $^{\circ}\text{C}$ )	293
Outlet Coolant temperature ( $^{\circ}\text{C}$ )	329

perturbations as a function of time. The modified CPAIR-P program is written in FORTRAN-77 for Personal Computers. After initialization, it calculates group constants using core design parameters (Table 3) in LEOPARD [30] program. The LEOPARD program is a zero-dimensional unit cell computer code with 54 fast and 172 thermal energy groups. Evaluated Nuclear Data (ENDF-IV) set has been used in the cross-section library. In this work, equivalent cells of a typical PWR [29] have been employed to generate group constants for fuel cells and water holes. These cell-averaged group constants are then used in the one-dimensional multi-group diffusion theory based ODMUG [31] code. The ODMUG calculates the group fluxes as a function of position in the reactor. These group fluxes are subsequently averaged over the core. Both LEOPARD and ODMUG are treated as subroutines of the CPAIR-P program. Then Eqs. (1)–(10) are solved using fourth-order Runge–Kutta method to find the activity values due to corrosion products in primary coolant, on piping, and on core surface. The program has three loops to study the corrosion rate changes, flow rate perturbations and activity due to each isotope with an overall loop over time steps.

### 3. Simulation results

A typical PWR [29] is considered with power of 1000 MWe and initial impurity concentrations taken to be zero. Experimental fractional exchange rates ( $\varepsilon_j Q_j / V_q$ ) and re-solution rates ( $K_j / V_q$ ) have been employed in the analysis [14] and are shown in Table 2. The design data values for a typical PWR are given as Table 3 [29]. The core averaged group fluxes have been

computed using LEOPARD and ODMUG codes. The plant surface area of about  $10^8 \text{ cm}^2$  is exposed to the primary coolant for corrosion and in the presence of corrosion inhibitors, an equilibrium corrosion rate of  $2.4 \times 10^{-13} \text{ g/cm}^2 \text{ s}$  [14,29] exists after one year of full power reactor operation. It has primary coolant volume of  $1.3 \times 10^7 \text{ cm}^3$ . The corrosion rate of  $25 \text{ }\mu\text{g/s}$  has been used as normal equilibrium value of corrosion rate in the subsequent studies.

The purification rate due to ion-exchanger,  $\varepsilon_1 Q_1$ , must be large enough to regard deposition, re-resolution and leakage as second-order effects. Therefore, using an approach as described in Ref. [17], an optimum removal rate of activity by the ion-exchanger was determined at a constant corrosion rate. It was found that saturation value of coolant activity remains fixed when  $\varepsilon_1 Q_1$  is more than  $400 \text{ cm}^3$  per second. Therefore, a conservative removal rate of  $600 \text{ cm}^3$  per second was selected for which the saturation value of activity is sufficiently low.

Six corrosion products ( $^{56}\text{Mn}$ ,  $^{24}\text{Na}$ ,  $^{59}\text{Fe}$ ,  $^{60}\text{Co}$ ,  $^{58}\text{Co}$  and  $^{99}\text{Mo}$ ) were considered in this study. During reactor operation at full power, the activity due to  $^{56}\text{Mn}$  remained the largest contributor to the total activity (Fig. 2). During normal operation, it has about 36% of the total corrosion product activity in the PWR whereas other isotopes including  $^{24}\text{Na}$ ,  $^{59}\text{Fe}$ ,  $^{99}\text{Mo}$  and  $^{60}\text{Co}$  contribute about 23.4%, 29.6%, 9.5% and 1.4% respectively. The activity due to  $^{56}\text{Mn}$  saturates at about 150 h after start of the reactor. It has saturation value of  $0.22 \text{ }\mu\text{Ci/cm}^3$  and due to it, the primary coolant activity rises to about 0.663 MCi source within 150–230 h of reactor operation at full power. The time variation of specific activity in primary coolant, on inner surfaces of pipes and on core surface is shown as Fig. 2 for  $^{60}\text{Co}$ ,  $^{56}\text{Mn}$  and  $^{24}\text{Na}$ . The activity on core surface and pipes due to cobalt remains high after shutdown (Fig. 2). The time variation of total activity due to all corrosion products is given as Fig. 3. During normal operation, the highest contributor to activity is scale on core surface and the second largest part comes from primary pipe scale. When reactor is shut down, the activity due to pipe scale becomes largest source and it decays slowly due to contributions of cobalt (Figs. 2 and 3). These are close to already reported values [32,33] in their source term measurements.

### 3.1. Constant corrosion rate and flow rate perturbations

Flow rate perturbations in a PWR can occur due to variations in the cross-sectional area of the flow channels or due to changes in primary pump speed. These perturbations subsequently affect temperatures, neutron flux in the core, corrosion production terms and loss terms. The load-following system then may try to adjust the flow rates in the reactor; however, if it cannot do so then the

reactor will scram. In this work, flow perturbations are introduced during the steady state operation of the reactor when corrosion products activity has reached its saturation value. Then corrosion product activity in coolant and pipe scale is observed using the CPAIR-P program.

A linear decrease in flow rate is introduced (at  $t = 500 \text{ h}$ ) for the reactor operating at full power under steady state conditions. In the transient, the corrosion products reach saturation values and the reactor is not allowed to undergo a scram. This linear decrease in flow rate is described by a parameter  $g(t)$ :

$$g(t) = \begin{cases} 1.0, & t < t_{\text{in}}, \\ 1.0 - \alpha(t_{\text{in}} - t), & t_{\text{in}} < t < t_{\text{max}}, \\ w_2/w_0, & t > t_{\text{max}}, \end{cases} \quad (11)$$

where  $\alpha$  is the slope of linear flow rate decrement and  $t_{\text{in}}$  is the time at which the perturbation in the mass flow rate is initiated. After time  $t_{\text{max}}$  the flow rate achieves a lower value of  $w_2$  as compared to  $w_0$ . Such a flow rate change affects  $T_c$  and  $T_L$  and therefore the effective neutron flux (Eq. (4)) gets modified, causing a change in the production rate of corrosion product activity.

In the first part of the study, the above parameter,  $g(t)$ , is introduced as a perturbation while the corrosion rate is kept constant. The flow rate is introduced at  $t_0 = 500 \text{ h}$  for various values of  $\Delta w$  for a period of 100 h. For constant corrosion rate in the system, the total specific activity in coolant, in the presence of flow rate perturbation, is shown in Fig. 4. As the flow rate decreases to about 10% of the rated value, the corrosion product specific activity attains a 14% higher new saturation value as shown in Fig. 4. It becomes 47% higher for a decrease of 30% in the flow rate. The total activity for core scale and pipe scale as a function of time are shown in Figs. 5 and 6 respectively. For a flow rate decrease of 10% ( $\Delta w = 0.1w_0$ ) the total activity on core surfaces increases to 14.6% higher value when compared to the corresponding value in the unperturbed state. It further increases to 58.2% larger activity on core surfaces when flow rate is reduced to  $0.7w_0$  during the perturbation.

The activity due to pipe scale rises slowly since long lived cobalt isotopes are the main contributors in this case. When the flow rate transient is introduced at  $t = 500 \text{ h}$  at constant corrosion rate, the resultant activity on pipe scale is shown in Fig. 6 for various flow changes ( $\Delta w$ ). The activity shows a small depression at the beginning of transient and then increases monotonically to higher saturation values. For a 10% decrease in flow rate, the saturation value of activity increases from  $1.78$  to  $1.97 \text{ }\mu\text{Ci/cm}^3$  (11% higher value). When the flow rate is allowed to decrease to  $0.7w_0$ , an increase of 37% in the saturation activity on pipe scale is observed. Such a hike in source will result in even larger

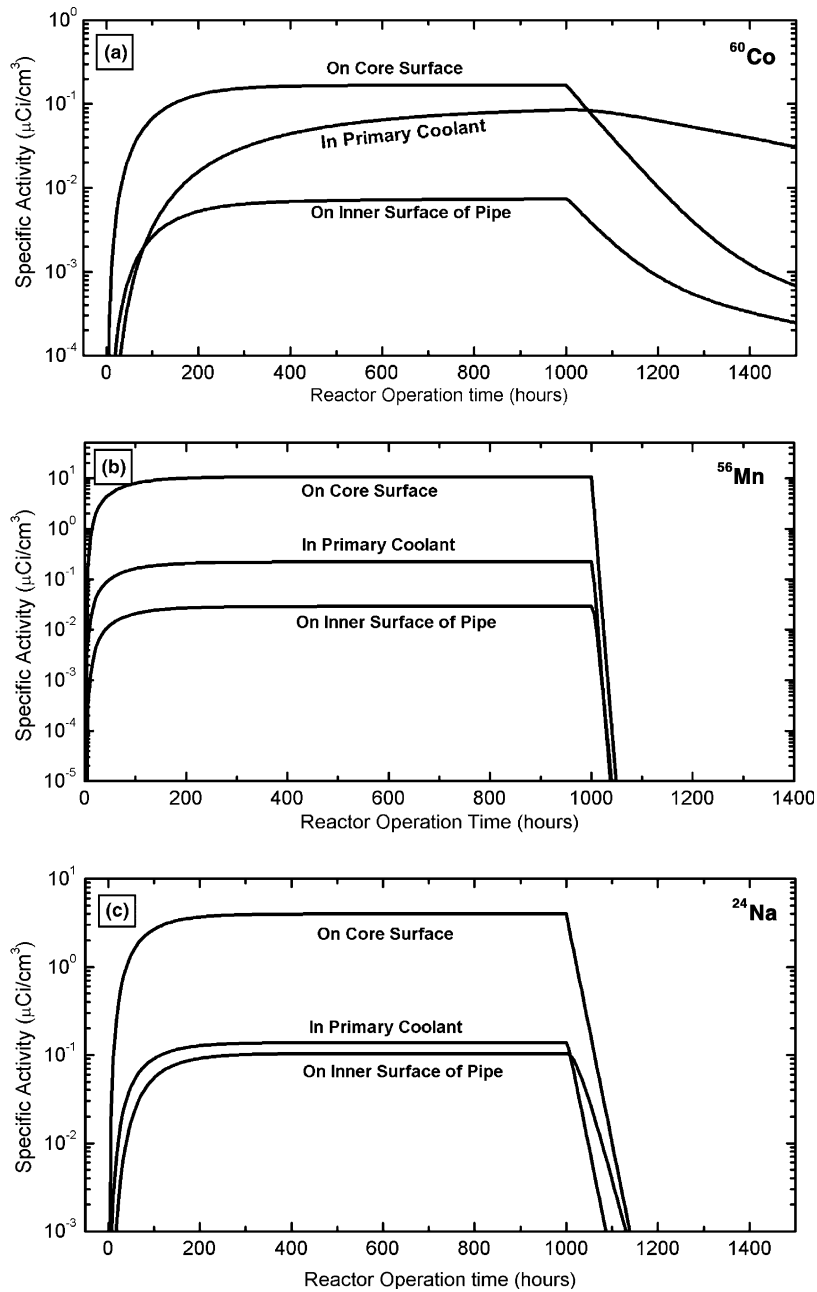


Fig. 2. Specific activity for (a)  $^{60}\text{Co}$ , (b)  $^{56}\text{Mn}$  and (c)  $^{24}\text{Na}$  in primary coolant, on inner surfaces of pipes and on core surfaces as a function of reactor operation time under normal conditions and constant corrosion rate (system shuts down at  $t = 1000$  h).

doses outside primary circuit near pump and heat exchanger.

### 3.2. Linear increase of corrosion rates

Slow and fast linear increase of corrosion rates have been studied using following model for time dependent corrosion rate  $C(t)$ :

$$C(t) = \begin{cases} 0, & t < a, \\ \frac{\Delta C}{\Delta t}(t - t_0), & a \leq t \leq b, \\ C_s, & t > b, \end{cases} \quad (12)$$

where  $\Delta C/\Delta t$  is a non-zero positive constant slope of corrosion rate in the time domain  $[a, b]$  and  $C_s$  is the equilibrium value of the rate after time 'b'. The time period 'a' is corrosion free time period prevailing for about

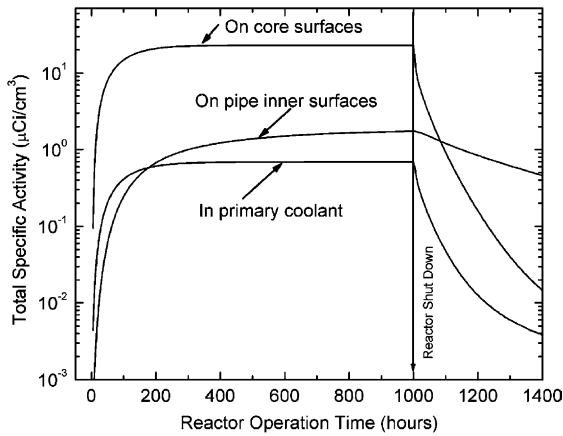


Fig. 3. Comparison of total specific activity due to corrosion products in primary coolant, on surfaces of pipes and core as a function of reactor operation time at full power under normal conditions and constant corrosion rate (system shuts down at  $t = 1000$  h).

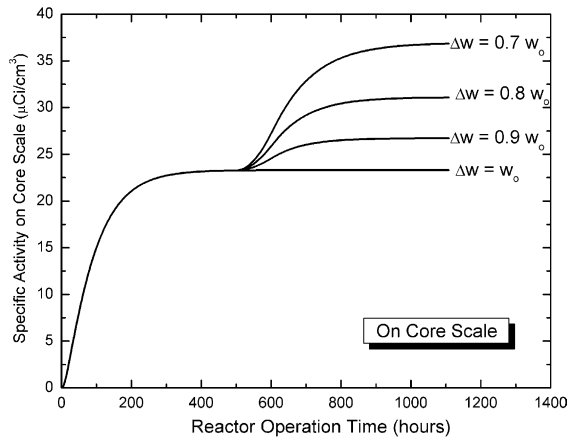


Fig. 5. Total specific activity due to corrosion products on core scale under linear flow rate perturbation for various  $\Delta w$  (initiated at  $t = 500$  h,  $\Delta t = 100$  h). Constant corrosion rate is assumed.

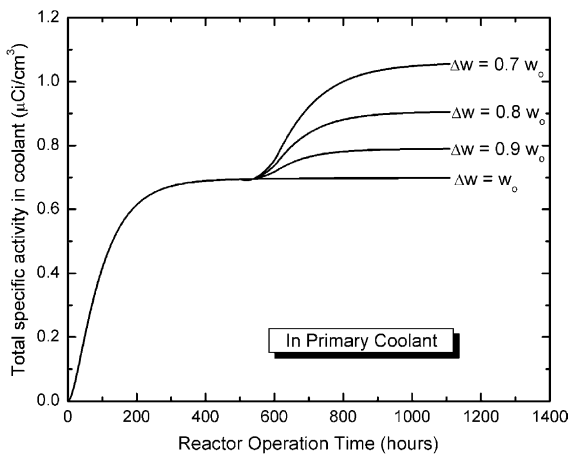


Fig. 4. Total specific activity due to corrosion products in primary coolant of a PWR under linear flow rate perturbation for various  $\Delta w$  (initiated at  $t = 500$  h,  $\Delta t = 100$  h). The corrosion rate is assumed to be constant and uniform.

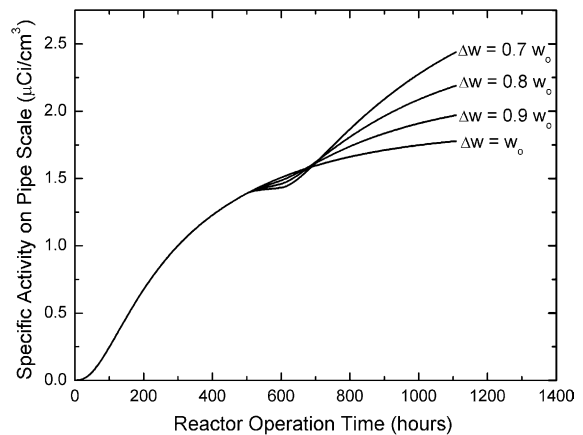


Fig. 6. Total specific activity due to corrosion products on primary pipe scale under linear flow rate perturbation for various indicated values of  $\Delta w$  (initiated at  $t = 500$  h,  $\Delta t = 100$  h). Constant corrosion rate is assumed.

50 h after the startup. When we introduce such a time dependent corrosion rate along with a flow rate perturbation, the resultant specific activity due to all corrosion products on pipe scale is shown in Fig. 7. For comparison, activities for constant carrier rate with and without a flow transient are also shown. The activity follows the corrosion rate curve having a value of slope in accordance with  $\Delta C/\Delta t$ . The linear flow rate perturbation (Eq. (11)) is introduced at  $t_0 = 500$  h. The activity in all cases eventually approaches a new saturation value. The time taken to reach the normal saturation value of  $1.55 \mu\text{Ci}/\text{cm}^3$  is relatively high. It increases with a de-

crease in  $\Delta C/\Delta t$  value as shown in Table 4. For a slow increase ( $\Delta C/\Delta t < 10^{-5} \mu\text{g}/\text{s}^2$ ), the time taken to reach the normal saturation value is about 938 h as compared to 650 h when a constant corrosion rate is used. These results suggest that effect of flow rate perturbations on specific activity due to pipe scale in the form of a dip in activity curve can be smeared by a linearly increasing corrosion rates. Such a dip can only be seen in activity when corrosion rate saturates to a constant value well before the initiation of the transient. The new saturation value depends on both the changes in flow rate ( $\Delta w$ ) and equilibrium for corrosion rate ( $C_s$ ).

The behavior of coolant activity on pipe scale has also been studied for a fixed corrosion increase at



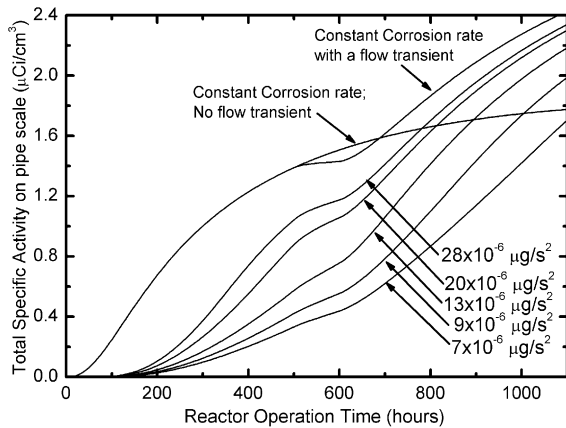


Fig. 7. Total specific activity due to corrosion products on primary pipe scale under linear flow rate transient ( $\Delta w = 0.3w_0$ ) initiated at  $t = 500$  h for various linearly rising corrosion rates with indicated values of slopes. Equilibrium corrosion rate remains fixed at  $25 \mu\text{g/s}$ .

Table 4

Time taken ( $t_s$ ) to reach normal saturation activity<sup>a</sup> as a function of  $\Delta C/\Delta t$  for a fixed linear flow rate transient<sup>b</sup>

$\Delta C/\Delta t$ ( $10^{-6} \mu\text{g/s}^2$ )	$t_s$ (h)
0.0	650
28	750
20	775
13	845
9	938
7	1045

<sup>a</sup> Total saturation activity value =  $1.55 \mu\text{Ci/cm}^3$  in primary pipe scale.

<sup>b</sup>  $\Delta w = 0.3w_0$  initiated at  $t = 500$  h for 100 h.

various equilibrium value ( $C_s$  from  $12.5$  to  $50 \mu\text{g/s}$ ) while the flow rate perturbation remain the same ( $\Delta w = 30\%$  of  $w_0$ , initiated at  $t = 500$  h for a period of 100 h). For such increase in corrosion rates, the resulting total specific activity on pipe scale is illustrated as Fig. 8. It is noticeable that the activity in the coolant attains new saturation value after the transient and this saturation value keeps on increasing with increase in equilibrium value ( $C_s$ ). These results indicate that new saturation activity after a flow rate transient depends on both the equilibrium value of corrosion rate ( $C_s$ ) and change in flow rate ( $\Delta w$ ). However, the time taken to reach the saturation activity depends on the slope of corrosion rate.

### 3.3. Effect of pump coastdown and linear corrosion increase

The primary pump coastdown due to a decrease in speed of a primary pump can be obtained by equating the frictional retarding force to the changes in the

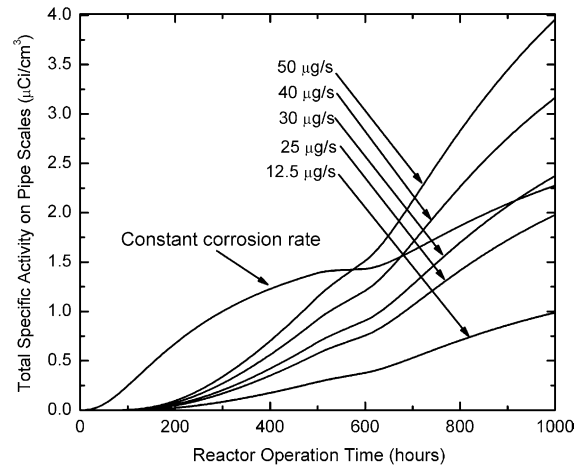


Fig. 8. Total specific activity due to corrosion products on primary pipe scale under linear flow rate transient ( $\Delta w = 0.3w_0$ ) initiated at  $t = 500$  h for various linearly rising corrosion rates with various indicated equilibrium values ( $\mu\text{g/s}$ ) and a fixed increase.

momentum of the fluid. The balance for a given average velocity ( $v$ ) and fluid density ( $\rho$ ) is given as [34]:

$$\frac{L\rho}{g_c} \frac{dv}{dt} = -C_f \frac{\rho v^2}{2g_c}, \quad (13)$$

where  $L$  is the total length of the loop and  $C_f$  is the total pressure loss coefficient for the loop. The solution in terms of flow rate is

$$w(t) = w_0 / (1 + t/t_p). \quad (14)$$

The time  $t_p$  is flow half-time ( $2L/C_f v_0$ ). An initial flow rate for steady state reactor operation is  $w_0$  and  $w(t)$  is flow rate at any time  $t$ . In this study, we considered  $t_p$  large enough so that the boiling crisis does not occur until after the reactor trip.

Using modified program CPAIR-P, the pump coastdown is introduced in the primary coolant circuit of a PWR for a given  $t_p$  value. Then specific activities in coolant and on pipe scale are estimated for both a constant corrosion rate and a linearly increasing corrosion. In this study we allowed slope of corrosion rate to vary in steps while keeping the equilibrium value fixed at  $25 \mu\text{g/s}$ . Results for primary coolant activity are shown in Fig. 9(a). For a constant corrosion rate, the flow coastdown is started at  $t = 50$  h after the reactor startup until the flow rate reaches 90% of the initial flow rate value and the reactor scrams. Total specific activity in the coolant approaches saturation value of  $0.67 \mu\text{Ci/cm}^3$  in accordance with increasing corrosion rates. For a case of linearly increasing corrosion rate with a pump coastdown, the coolant activity monotonically rises and follows the slope of corrosion rate. If the slope is greater than  $9 \times 10^{-6} \mu\text{g/s}^2$ , then activity crosses the normal

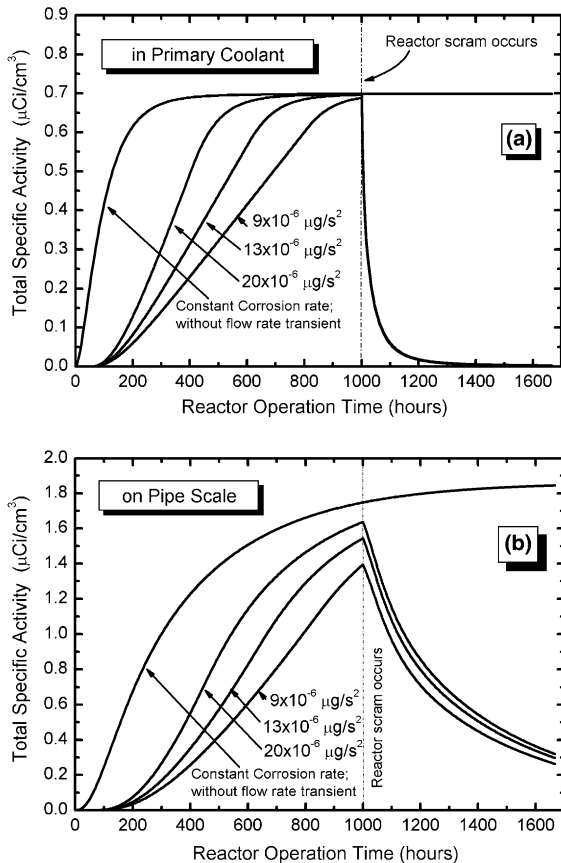


Fig. 9. Total specific activity due to corrosion products in primary coolant (a) and on primary pipe scale (b) under pump coastdown ( $t_p = 2000$  h) initiated at  $t = 500$  h for various indicated linearly rising corrosion rates. Reactor was allowed to scram at 90% of its rated flow rate.

saturation value of  $1.55 \mu\text{Ci}/\text{cm}^3$  before the reactor scram occurs. Total specific activity on pipe scale rises slowly and for slow increase in corrosion it does not reach saturation value of  $1.55 \mu\text{Ci}/\text{cm}^3$  (Fig. 9(b)). The peak values have been found to depend on the values of corrosion rate. The peak value and decay of activity after scram are strong function of flow rate and efficiencies to remove activity from pipe scale.

#### 4. Conclusions

For linearly increasing corrosion rates, the transient behavior of corrosion product activity has been studied for a typical pressurized water reactor (PWR) under flow rate perturbations. For this purpose, the computer program CPAIR-P [27] has been modified to accommodate for a time dependent linear corrosion rate model. Results for transient response of concentrations of  $^{24}\text{Na}$ ,  $^{56}\text{Mn}$ ,  $^{59}\text{Fe}$ ,  $^{58}\text{Co}$ ,  $^{60}\text{Co}$  and  $^{99}\text{Mo}$  show that the

specific activity in primary loop approaches equilibrium value under normal operating conditions fairly rapidly. Predominant corrosion product activity during operation is due to  $^{56}\text{Mn}$  where as the  $^{58}\text{Co}$  and  $^{60}\text{Co}$  dominate it after shut down. Then flow rate perturbations were simulated for various linearly increasing corrosion rates and their effect on saturation activity was studied. For a linear decrease in flow rate and at a constant corrosion rate, the total coolant activity and activity on pipe scale approaches to higher saturation values. For a linearly increasing corrosion the activities in the coolant, on core surfaces and on pipe scale attain new saturation values after the transient and these saturation values keep on increasing with an increase in equilibrium value ( $C_s$ ). The results show that the effect of flow rate perturbations on specific activity due to pipe scale in the form of a dip in activity curve is smeared by linearly rising corrosion rates. The new saturation activity after a flow rate transient depends on both the equilibrium value of corrosion rate ( $C_s$ ) and the change in flow rate ( $\Delta w$ ). The time taken to reach the saturation activity depends on the slope of corrosion rate. The peak value and decay of activity after scram have been found to depend on flow rate and removal efficiencies of isotopes from pipe scale.

#### Acknowledgment

M. Rafique gratefully acknowledges the financial support of the Higher Education Commission (HEC), Pakistan for the PhD (Indigenous) fellowship under Grant # 17-6 (097) Sch/2001/4806.

#### References

- [1] IAEA, High Temperature On-Line Monitoring of Water Chemistry and Corrosion Control in Water Cooled Power Reactors, IAEA-TECDOC-1303, Vienna, 2002.
- [2] T. Moore, EPRI J., November 1984.
- [3] G. Choppin, J. Rydberg, J.O. Liljenzin, Radiochemistry and Nuclear Chemistry, Butterworth-Heinemann, Oxford, 1995.
- [4] D. Bodansky, Nuclear Energy – Principles, Practices and Prospects, AIP, Woodbury, NY, 1996.
- [5] J.W. Cleaver, B. Yates, J. Coll. Interf. Sci. 44 (1975) 464.
- [6] F.P. Berger, K. Hau, Int. J. Heat Mass Transfer 20 (1977) 1185.
- [7] P. Beslu, Proceedings of the International Conference on Water Chemistry of Nuclear Reactor Systems, Bournemouth, BNES, London, 1978.
- [8] S. Kang, EPRI NP-4246, 1985.
- [9] C.B. Lee, PhD thesis, Nucl. Eng. Dept., MIT, 1990.
- [10] P.J. Millet, C.J. Wood, EPRI, Proceedings of 58th International Water Conference, Pittsburg, 1997.

- [11] G.R. Dey, D.B. Naik, K. Kishore, C.K. Vinayakumar, B. Yuvaraju, G. Venkateswaran, P.N. Moorthy, *Radiat. Phys. Chem.* 52 (2) (1998) 171.
- [12] G. Hirschberg, P. Baradlai, K. Varga, G. Myburg, J. Schunk, P. Tilky, P. Stoddart, *J. Nucl. Mater.* 265 (3) (1999) 273.
- [13] K. Varga, G. Hirschberg, Z. Németh, G. Myburg, J. Schunk, P. Tilky, *J. Nucl. Mater.* 298 (3) (2001) 231.
- [14] R.G. Jaeger (Ed.), *Engineering Compendium on Radiation Shielding*, vol. III, Springer-Verlag, New York, 1970.
- [15] N.M. Mirza, A.M. Mirza, T.M. Qaisrani, N. Ahmad, *The Nucleus* 263 (4) (1989) 23.
- [16] N.M. Mirza, S.M. Mirza, N. Ahmad, *Nucl. Technol.* 96 (3) (1991) 237.
- [17] A.M. Mirza, N.M. Mirza, I. Mir, *Ann. Nucl. Energy* 25 (6) (1997) 331 (Volume date 1998).
- [18] A. Raymond, A. de Murcia, S. Dhaunut, *Anal. Chem. Acta* 195 (1987) 265.
- [19] N.M. Mirza, S.M. Mirza, *Nucl. Energy (Br. Nucl. Energy Soc.)* 32 (6) (1993) 387.
- [20] N.M. Mirza, S.M. Mirza, *Ann. Nucl. Energy* 20 (6) (1993) 381.
- [21] N.M. Mirza, S.S. Chughatai, N. Ahmad, L.A. Khan, *Nucl. Sci. J.* 34 (3) (1997) 203.
- [22] M. Iqbal, N.M. Mirza, S.M. Mirza, S.K. Ayazuddin, *Ann. Nucl. Energy* 24 (3) (1996) 177 (volume date 1997).
- [23] M. Iqbal, N.M. Mirza, S.M. Mirza, *Nucl. Sci. J.* 35 (2) (1998) 81.
- [24] A.M. Mirza, S. Khanam, N.M. Mirza, *Ann. Nucl. Energy* 25 (18) (1998) 1465.
- [25] R. Nasir, N.M. Mirza, S.M. Mirza, *Ann. Nucl. Energy* 26 (17) (1999) 1517.
- [26] R. Khan, N.M. Mirza, S.M. Mirza, *Nucl. Sci. J.* 36 (1) (1999) 27.
- [27] F. Deeba, A.M. Mirza, N.M. Mirza, *Ann. Nucl. Energy* 26 (7) (1999) 561.
- [28] M.G. Fontana, *Corrosion Engineering*, 3rd Ed., McGraw-Hill, Singapore, 1987.
- [29] S. Glasstone, A. Sesonske, *Nuclear Reactor Engineering*, Von Nostrand, New York, 1981.
- [30] R.F. Barry, WCAP-3269-26, Westinghouse Electric Corporation, 1963.
- [31] J.R. Thomas, H.C. Edlund, *Proceedings of the Conference ICTP, Trieste*, 1980.
- [32] J.W. Mandler et al., NUREG/CR-4397, US Nuclear Regulatory Commission, 1985.
- [33] P.G. Volleque, *Nucl. Technol.* 90 (1990) 23.
- [34] E.E. Lewis, *Nuclear Power Reactor Safety*, John Wiley, New York, 1977.